

2000

Modeling of Metal(100) Homepitaxial Film Growth at Very Low Temperatures

K. J. Caspersen
Iowa State University

C. R. Stoldt
Iowa State University

Patricia A. Thiel
Iowa State University, thiel@ameslab.gov

James W. Evans
Iowa State University, evans@ameslab.gov

Follow this and additional works at: http://lib.dr.iastate.edu/ameslab_conf

 Part of the [Chemistry Commons](#), and the [Materials Science and Engineering Commons](#)

Recommended Citation

Caspersen, K. J.; Stoldt, C. R.; Thiel, Patricia A.; and Evans, James W., "Modeling of Metal(100) Homepitaxial Film Growth at Very Low Temperatures" (2000). *Ames Laboratory Conference Papers, Posters, and Presentations*. 63.
http://lib.dr.iastate.edu/ameslab_conf/63

This Conference Proceeding is brought to you for free and open access by the Ames Laboratory at Iowa State University Digital Repository. It has been accepted for inclusion in Ames Laboratory Conference Papers, Posters, and Presentations by an authorized administrator of Iowa State University Digital Repository. For more information, please contact digirep@iastate.edu.

Modeling of Metal(100) Heteroepitaxial Film Growth at Very Low Temperatures

Abstract

We model the growth of Ag films deposited on Ag(100) below 140K. Our recent Variable-Temperature Scanning Tunneling Microscopy (VTSTM) studies reveal “smooth growth” from 120-140K, consistent with earlier diffraction studies. However, we also find rougher growth for lower temperatures. This unexpected behavior is modeled by describing the deposition dynamics using a “restricted downward funneling” model, wherein deposited atoms get caught on the sides of steep nanoprotusions (which are prevalent below 120K), rather than always funneling down to lower four-fold hollow adsorption sites. At OK, where no thermal diffusion processes are operative, this leads to the formation of *overhangs and internal defects* (or *voids*). Above 40K, low barrier interlayer diffusion processes become operative, producing the observed smooth growth by 120K. We also discuss how the apparent film morphology mapped out by the STM tip “smears” features of the actual film morphology (which are small at low temperature), and also can lead to underestimation of the roughness.

Disciplines

Chemistry | Materials Science and Engineering

Comments

This article is from *Recent Developments in Oxide and metal Epitaxy: Proceedings of the MRS 2000 Spring Meeting* 619 (2000): pp. 49—54, doi:[10.1557/PROC-619-49](https://doi.org/10.1557/PROC-619-49)

MODELING OF METAL(100) HOMOEPITAXIAL FILM GROWTH AT VERY LOW TEMPERATURES

K.J. CASPERSEN¹, C.R. STOLDT^{1*}, P.A. THIEL¹, and J.W. EVANS²
Departments of Chemistry¹ and Mathematics², and Ames Laboratory,
Iowa State University, Ames, Iowa 50011

ABSTRACT

We model the growth of Ag films deposited on Ag(100) below 140K. Our recent Variable-Temperature Scanning Tunneling Microscopy (VTSTM) studies reveal "smooth growth" from 120-140K, consistent with earlier diffraction studies. However, we also find rougher growth for lower temperatures. This unexpected behavior is modeled by describing the deposition dynamics using a "restricted downward funneling" model, wherein deposited atoms get caught on the sides of steep nanoprotusions (which are prevalent below 120K), rather than always funneling down to lower four-fold hollow adsorption sites. At 0K, where no thermal diffusion processes are operative, this leads to the formation of *overhangs* and *internal defects* (or *voids*). Above 40K, low barrier interlayer diffusion processes become operative, producing the observed smooth growth by 120K. We also discuss how the apparent film morphology mapped out by the STM tip "smears" features of the actual film morphology (which are small at low temperature), and also can lead to underestimation of the roughness.

I. INTRODUCTION

Traditionally, the roughness of deposited homoepitaxial films (of a given thickness) was expected to increase with decreasing temperature (T), due to enhanced kinetic barriers to smoothing [1,2]. One well-known exception is "re-entrant" smooth growth at low T in the Pt/Pt(111) system [3], but this behavior is due to a transition from compact to fractal islands (which facilitates downward transport). Perhaps more surprising is the "smooth growth" at liquid nitrogen temperatures observed in diffraction studies [4,5] of metal(100) homoepitaxial growth, for which there is no analogous island shape transition. This smooth growth, and observed long-range lateral spatial correlations (i.e., narrow diffraction profiles) in the submonolayer regime, were associated with "transient mobility" of "hot" deposited adatoms (noting that thermal terrace diffusion is inoperative at low T) [4]. Such transient mobility was not found in molecular dynamics (MD) studies [6], and instead it was proposed that smooth growth was due to "downward funneling" of depositing atoms to lower four-fold hollow sites in the fcc(100) geometry [6]. The narrow profiles have been attributed to intralayer "clumping" of atoms deposited nearby other adatoms facilitated by low-barrier edge diffusion processes [7].

Our recent VTSTM studies [8] of the morphology of 25ML Ag films deposited on Ag(100) do in fact find "re-entrant" smooth growth (i.e., roughness increases as T is lowered to 220K, but then decreases again until 140K). This is consistent with the earlier diffraction studies [4,5]. However, our studies also reveal rougher growth for lower T, the explanation of which is the focus of this paper. Motivated in part by recent MD studies [9], we propose that the latter feature is due to "restricted downward funneling (RDF)", where deposited atoms get caught on the sides of steep nanoprotusions (which are prevalent below 120K). In Sec.II, we analyze this model for growth at 0K. Next, in Sec.III, we introduce certain low-barrier thermal diffusion processes that are operative above 40K. This reproduces the additional smoothing observed experimentally by 120K. Some discussion of model behavior is provided in Sec.IV. In Sec.V, we compare the actual film morphology with that probed by STM tip. Conclusions are provided in Sec. VI.

We focus on the behavior of the surface roughness, W , of the growing film. Let P_j denote the (normalized) population in layer j of "surface atoms", by which we mean those atoms which are at the top of each vertical column of atoms in the fcc(100) geometry. Then, one has $W^2 = \sum_j (j-j_{av})^2 P_j$, where $j_{av} = \sum_j j P_j$ is a measure of the mean film height. This W is measured in units of the interlayer spacing, $b = 2.04 \text{ \AA}$ for Ag(100). One can also consider the skewness, $\kappa = W^{-3} \sum_j (j-j_{av})^3 P_j$, and the kurtosis, $Q = W^{-4} \sum_j (j-j_{av})^4 P_j - 3$ (which measures the amount of the height distribution in the tail, relative to a Gaussian distribution).

II. "RESTRICTED DOWNWARD FUNNELING" MODEL FOR GROWTH AT 0K

The idea behind this model is that depositing atoms can be captured or trapped at sites with:

- (i) four supporting atoms, i.e., four-fold hollow adsorption sites in the fcc(100) geometry;
- (ii) three supporting atoms, i.e., one supporting atom is "missing" compared with (i);
- (iii) two supporting atoms, provided there are one (or more) in-layer neighbors;
- (iv) one supporting atom, provided there are two (or more) in-layer neighbors.

More specifically, in the RDF model, an atom impinging on the surface funnels downward until reaching one of the above trap sites. In contrast, for pure downward funneling (DF), the atom continues further down until reaching a four-fold hollow site. See Fig. 1 for schematics of DF, RDF, and the above trap sites. Note that in the RDF model of homoepitaxial growth, the formation of overhangs and internal defects or voids is possible, as seen in MD studies [9].

Next, we consider the behavior of the roughness, W , for the growing film. Fig.2a shows W versus the thickness or coverage, θ (in monolayers, ML), for RDF and for DF. For a 25ML film,

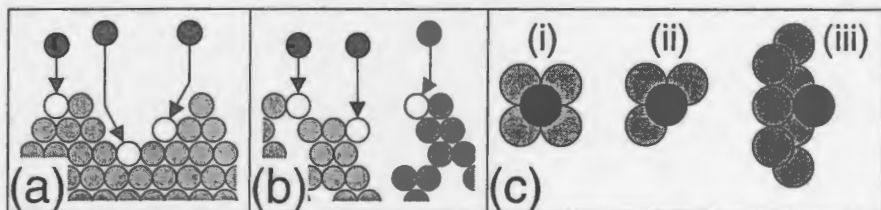


Fig.1. 1+1 dimensional schematics of: (a) downward funneling; (b) restricted downward funneling; (c) bird's eye view of trap sites (black circles) of types (i)-(iii).

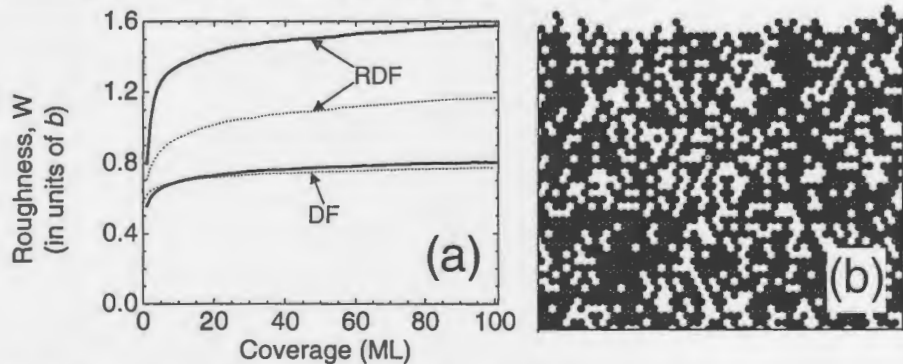


Fig.2. (a) Roughness, W , versus θ for RDF and DF. The *thin* dotted lines show W estimated by the STM tip (see Sec.V). (b) Cross-section of a film grown by RDF.

one finds for RDF that $W^{RDF} = 1.41 b$ versus a much smaller $W^{DF} = 0.74 b$ for standard DF. The defect density of thick (100ML) films is 28.4% for RDF (versus 0% for DF). See Fig. 2b.

III. GROWTH BETWEEN 0K AND 140K: LOW-BARRIER INTERLAYER DIFFUSION

The next challenge is to extend the RDF model to describe the T-dependence growth (and specifically of W) up to 140K where terrace diffusion is still inoperative. (The barrier for terrace diffusion is 0.4eV with a prefactor of $10^{13} s^{-1}$, implying a hop rate below $0.04 s^{-1}$ at 140K.) The key point to be made here is that on the irregular structures formed during film growth at low T, there are many other thermally activated *interlayer* hopping processes with low barriers, E_{act} , which can be operative and affect film morphology. For example, consider a "micropyramid" with sides corresponding to $\{111\}$ microfacets. Atoms on such facets are thermally mobile even down to 40K [1], which can lead to a novel downward transport pathway.

With this in mind, we have augmented the above RDF model by incorporating various interlayer hopping processes for atoms with low coordination number, m , as follows: hopping is instantaneous for $m < 3$; $E_{act} = 0.10 eV$ for $m = 3$ (or 0.15eV for three supporting atoms); $E_{act} = 0.25 eV$ for interlayer hops with $m = 4$ and 5. See Fig.3. Attempt frequencies are set to $10^{12} s^{-1}$. These choices are motivated by the known attempt frequency and terrace diffusion barrier (0.10eV) for Ag/Ag(111) [1], and by semi-empirical studies of other activation barriers. Terrace diffusion, involving hopping out of four-fold hollow sites, is still inoperative. One other significant choice in the model is whether to allow adatoms to pass through sites with low coordination, as e.g., is necessary to hop from the $\{111\}$ -faceted sides of a mesa-like microprotrusion to the top. Our model I has no restriction on the coordination of sites visited, and thus allows climbing "up and over". In contrast, in our model II, sites visited must have coordination $m > 2$, which forbids climbing up on top of mesas, so adatoms diffuse "up and back". The latter is consistent with the additional "large" step-edge barrier which exists at the edge of Ag islands on Ag(111).

As T increases from 0K, these interlayer diffusion processes turn on in sequence according to the hierarchy of energetic barriers. This leads to the step-wise variation of W versus T for a 25ML film shown in Fig. 4 for an (experimental) deposition flux of $F = 0.040 ML/s$. Our models recover the general trend in the experimental data (also shown) between 50K and 135K. Note that in model I, W does not always decrease with increasing T. This is due to the fact that activation of certain interlayer diffusion processes can lead to some atoms climbing uphill rather than downhill. From the simulations, we also extract the T-dependence of other aspects of film morphology, e.g., the density of internal defects (Fig.5a), and the skewness and kurtosis of the surface (Fig.5b) of 25ML films. The negative skewness and positive kurtosis for low T correspond to a film surface with deep narrow crevasses, a feature which disappears at higher T.

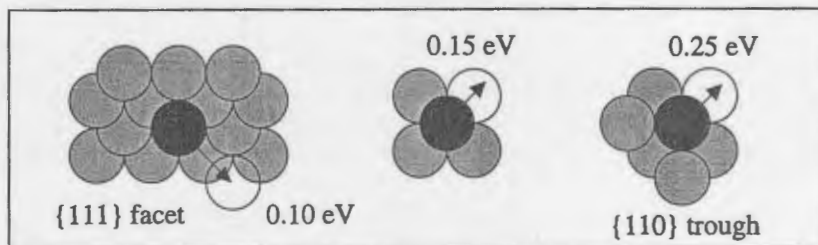


Fig.3. Bird's eye view of various low-barrier interlayer diffusion processes: hopping on a $\{111\}$ microfacet; hopping down from a site with three supporting atoms; hopping down a $\{110\}$ type trough.

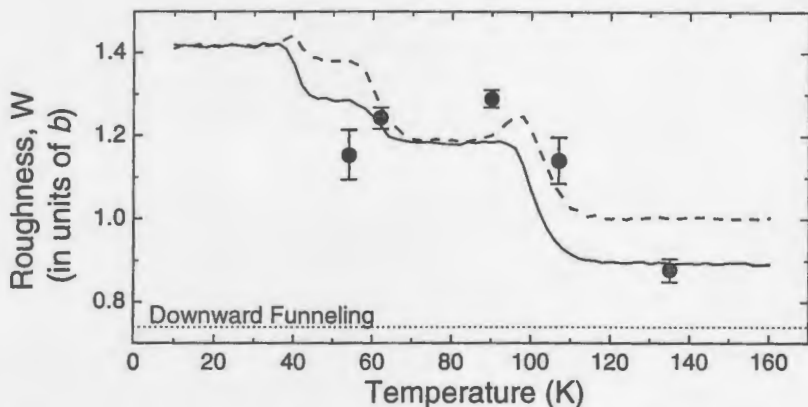


Fig.4. W versus T for a 25ML film according to model I (dashed line) and model II (solid line), with the choice of barriers indicated in Fig.3 and the text. Symbols denote experimental estimates of W , with error bars indicating the statistical uncertainty. In all cases, $F=0.040\text{ML/s}$.

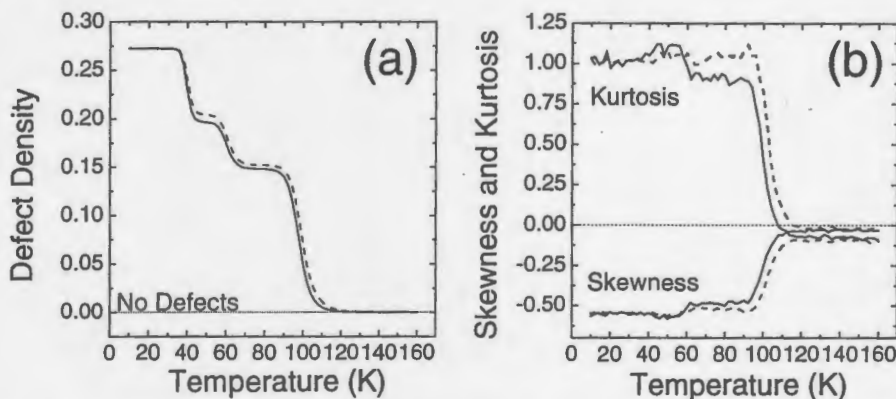


Fig.5. Temperature dependence for 25ML films of: (a) the density of internal defects; (b) the skewness and kurtosis. Results are shown for model I (dashed line) and model II (solid line).

Thus, a picture emerges that idealized DF provides a reasonable description of deposition dynamics at temperatures above 100K, because either the film morphology is locally smooth enough to make breakdown of DF rare, or when breakdown occurs, low barrier interlayer diffusion processes are active can bring deposited atoms to lower 4FH sites.

IV. DISCUSSION

To elucidate the behavior of film growth, one can consider a coarse-grained description of the evolution of the film height, $h(\underline{x}, t)$, at various lateral positions, \underline{x} , according to

$$\partial/\partial t h = F/\rho - \nabla \cdot \underline{J} + \eta, \quad (1)$$

where F is the deposition flux, ρ is the film density ($\rho=1$ being defect free), \underline{J} is the lateral mass flux of adatoms on the surface, and η is the uncorrelated deposition noise. For the DF model, one has $\rho=1$ and $\underline{J} \approx -cF\nabla h$, so (1) becomes the linear Edwards-Wilkinson equation [7,10]. Here W increases logarithmically with $\theta=Ft$, and the skewness and kurtosis vanish. For RDF, one has $\rho < 1$, and furthermore expects that $\rho = \rho_0(1+d|\nabla h|^2)$. Since \underline{J} should retain the form for DF with reduced c (due to reduced downward funneling), then (1) adopts the non-linear KPZ form. For 2+1 dimensional models in the KPZ-class such as RDF for 0K growth, random deposition at four-fold hollow sites (RD4FH) [10] and ballistic deposition [BD], one expects that $W \sim \theta^\beta$ with $\beta \approx 0.24$. This applies in the experimentally relevant coverage range for RD4FH, but not for RDF where the effective $\beta \approx 0.06$ at 100ML (or for BD). We presume that this is in part because of a very weak non-linearity for RDF with $d \approx -0.081$. The feature of a very slow crossover to true asymptotic KPZ behavior is familiar from studies of other growth models with internal defects [11]. However, all these models display similar behavior of the skewness, κ (kurtosis, Q), which vary from -0.55 to -0.44 (1.03 to 0.74) for RDF, -0.38 to -0.41 (0.26 to 0.32) for RD4FH, and -0.70 to -0.33 (1.78 to 1.04) for BD in the 25-100ML range. For the models of Sec.III incorporating interlayer diffusion, behavior for higher T (around 140K) is similar to that for pure downward funneling. This highlights the fact that thermal diffusion on the surface is still limited, not including terrace diffusion or detachment from step edges (which produce rather different behavior). In all these models, the above equation predicts self-affine morphologies for the growing film, consistent with experimental observations and with simulations.

V. TIP-PROBED VERSUS ACTUAL FILM MORPHOLOGY

Finally, we comment on a generic issue as regards using STM to probe film morphology. For low temperatures, where the film surface has small, steep nanoprotusions, one expects that the STM tip can not fully probe the surface, and thus produces a mollified morphology. In particular, one expects that the roughness, W , can be underestimated. To illustrate this point, we also show in Fig.2 the reduced W for the RDF model of growth at 0K, as measured by a conical tip with slope $s = \Delta y / \Delta x = 1$. (In this analysis, the tip is lowered at each point, x , above the surface until it contacts the surface. See Fig. 6.) Another perspective comes from comparing the actual morphology of a simulated film, the modified morphology of the simulated film mapped out by conical STM tips with various apex angles, and an actual VTSTM image of a film grown at the same T . This is done in Fig.7 for film growth at about 50K, where we note that the simulated morphology from a tip a fifth as steep as that used above reasonably reflects the actual measured experimental morphology.

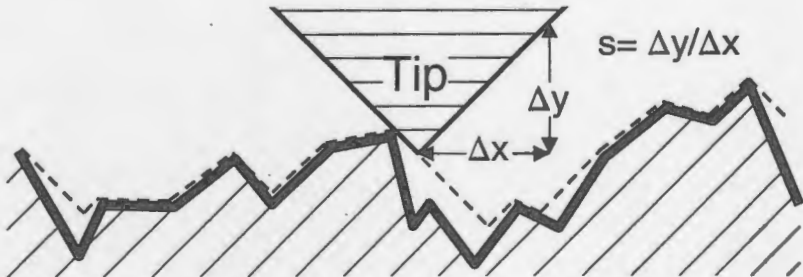


Fig 6. Schematic of a STM scan: solid dark line represents the real surface; dashed line represents the surface mapped out by the STM tip.

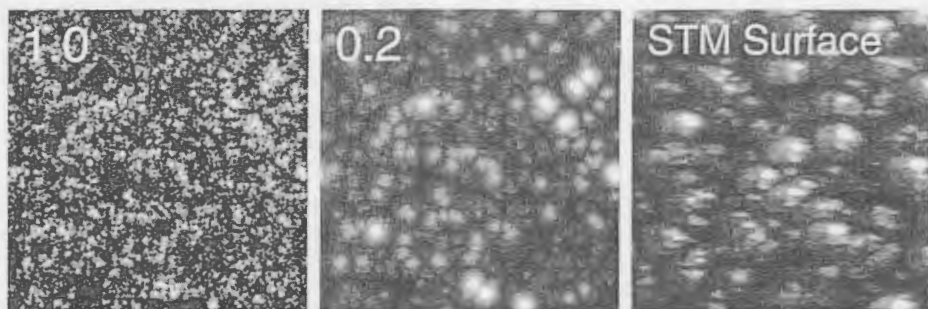


Fig.7. Comparison of simulated tip-mapped and STM morphologies. s -values are shown.

VI. CONCLUSIONS

Our simple RDF model, augmented by low-barrier interlayer diffusion processes, succeeds in producing the basic behavior observed by VTSTM for the roughness of Ag films deposited on Ag(100) between 50K and 140K. Of course, various refinements of the model are possible to incorporate, e.g., some downward funneling from the trap sites with less than four supporting atoms, "knockdown" of incompletely supported adatoms by depositing atoms, intralayer edge diffusion, and a more accurate and diverse selection of barriers of interlayer diffusion processes. However, we believe that our simplified model captures the essential features of low T growth.

ACKNOWLEDGEMENTS

This work was supported by NSF Grant CHE-9700592, and performed at Ames Laboratory which is operated for the USDOE by Iowa State University under Contract No. W-7405-Eng-82.

*Current address: Department of Chemical Engineering, University of California, Berkeley, CA 94720

REFERENCES

1. *Morphological Organization in Epitaxial Growth and Removal*, edited by Z. Zhang and M.G. Lagally (World Scientific, Singapore, 1998)
2. Another inappropriate view found in Ref.[1] is that smoother growth at low T is simply due to the presence of smaller islands from which deposited atoms can more easily descend; cf. Ref.[8].
3. R. Kunkel, B. Poelsema, L.K. Verheij, and G. Comsa, *Phys. Rev. Lett.* **65**, 733 (1990).
4. W.F. Egelhoff and I. Jacob, *Phys. Rev. Lett.* **62**, 921 (1989).
5. D.K. Flynn-Sanders, J.W. Evans, and P.A. Thiel, *Surf. Sci.* **289**, 77 (1993); *J. Vac. Sci. Technol. A* **7**, 2162 (1989).
6. J.W. Evans, D.E. Sanders, P.A. Thiel, and A.E. DePristo, *Phys. Rev. B* **41**, 479 (1990).
7. M.C. Bartelt and J.W. Evans, *Surf. Sci.* **423**, 189 (1999); G. Vandoni, C. Felix, R. Monot, J. Buttet, W. Harbich, *Surf. Sci.* **320**, L63 (1994); M. Breeman, unpublished.
8. C.R. Stoldt, K.J. Caspersen, M.C. Bartelt, C.J. Jenks, J.W. Evans, and P.A. Thiel, *Phys. Rev. Lett.*, submitted (2000).
9. C. Kelchner and A.E. DePristo, *Surf. Sci.* **393**, 72 (1997).
10. H.C. Kang and J.W. Evans, *Surf. Sci.* **271**, 321 (1992)
11. M. Schimschak and J. Krug, *Phys. Rev. B* **52**, 8550 (1995); S. Das Sarma, C.J. Lanczycki, S.V. Ghaisas, and J.M. Kim, *Phys. Rev. B* **49**, 10693 (1994).